HiSST: International Conference on
High-Speed Vehicle Science Technology
26–29 November 2018, Moscow, Russia

Comprehensive Effect of Secondary Heat Release on the ejection and engine performance in RBCC ejector mode

Pan Hongliang[1], *Lin Binbin*[1,2], *Ye Jinying*[3]

Abstract

In order to improve RBCC engine's specific impulse in the case of a high propellant consumption by inserted rocket in RBCC ejector mode, thrust augmentation relies on secondary fuel burning with incoming air. Because of complex mechanism in flow and combustion in ejector mode, effective ejection and secondary burning has to be matched in coupling with the primary rocket jet, incoming airflow and configuration of ramjet combustor. In the paper three-dimensional CFD and ground direct-connect experiments have been undertaken to study effects of combustion organization on ejection and engine performance. A steady burning and thermal choke have been realized through pylon and cavity aided combustion organization in a range of 0.4~0.8kg/s of rocket flow rate at flight Ma2. It is found that bypass ratio is not a unique seeking factor for high engine performance in ejector mode. RBCC engine performance improvements rely on a thermal choke position downstream rather than on a bypass ratio. The feasibility to improve specific impulse has also been studied through increase of secondary fuel equivalence ratio by means of rocket throttling.

Keywords: *RBCC, Ejector Mode, Secondary Combustion, Bypass Ratio, Engine performance*

1. Introduction

RBCC is a rocket based combined cycle propulsion system. It consists of parallel thrust units. In each unit, one or more primary rockets locates along the ram inner flow path. At static state and low flight Ma, the rockets produce thrusts, and meanwhile entrain air into RBCC ram inner flow path which is referred to an ejection, exactly to an ejector-suction during low Ma flights. The ejection is valued according to a bypass ratio defined as a mass flow rate ratio of the incoming air to the rocket jets. With flight Ma increases, ejection is enhanced because of ejector-ramjet effect even if the inlet unstart. Additional thrusts are hereby produced through organizing so called secondary burning between incoming air and injected secondary fuel in thrust units, and the engine thrust is a sum of that of all units produced by all inserted rockets jets, and also by all the secondary burning as well. Such RBCC operation range is recognized as in its ejector mode, and enables a flight vehicle to take off from static state by self-acceleration and return to base site with propulsion regulating. Herein RBCC makes self-acceleration and reusable launch possible, and has a wider envelop than ramjets and scramjets. Unfortunately half of propellants are consumed in ejector mode, according to a trajectory analysis when RBCC used as the first propulsion of two-stage-to-orbit [1]. The high consumption of propellants in ejector mode lowers specific impulse of whole trajectory of RBCC, and restricts competitiveness of self-acceleration RBCC to a certain extent.

Many efforts have made to improve RBCC performance in ejector mode. As studied by Lin and Pan through thermodynamic cycle analysis [2], thrust augmentation (RBCC thrust increase amount in terms of the primary rocket thrust under identical operating conditions) is achieved only if a secondary burning is organized. Also Etele confirmed that increase of thrust from incoming air is a benefit for RBCC performance in ejector mode [3] and influenced by thermodynamic cycle efficiency and bypass ratio as well [4]. Obviously effective ejection and secondary heat release are critical for a high specific impulse. Studies [5] [6] have made through optimizing rocket jet operation in ejector mode in order to achieve a

[1] *Science and Technology on Combustion, Internal Flow and Thermo-structure Laboratory, Northwestern Polytechnical University, Xi'an, China, 710072, panhl@nwpu.edu.cn*
[2] *Civil Aviation Flight University of China, GuangHan, China, 618307, linbb33@163.com*
[3] *Science and Technology on Combustion, Internal Flow and Thermo-structure Laboratory, Northwestern Polytechnical University, Xi'an, China, 710072, yejinying@mail.nwpu.edu.cn*

high bypass ratio. The inner flow path configuration has to be considered in rocket operation. An inserted rocket is constrained in its exit area in RBCC ram inner flow path and a blockage ratio is usually taken as a value of about 0.3, which is defined as the exit area of the rocket to the section area of combustor. Then it is important to avoid a deep under-expanding of a rocket jet, which may cause Fabri choking [7] [8] and diminish the bypass ratio. Studies show that a higher rocket chamber pressure is benefit for improving bypass ratio and engine performance [2] [9]. Also it is found that bypass ratio increases with the rocket mixture ratio when no secondary burning. The greatest engine performance is obtained at Ma2 with thrust argumentation 36.5%, when rocket is at an equivalence mixture ratio. On contrast, increasing ram combustor pressure through the second burning results in a bypass ratio decrease.

On the other hand, high bypass ratio related incoming air relies on a stable and efficient burning with secondary fuel to derive the secondary heat release. For a wide operating RBCC with fixed combustor geometry, its ram inner flow path is configured as a slight divergent, and is feasible in a scramjet mode directly to accelerate gas mixture further before entering the aft nozzle. In a ramjet- and ejector mode, a thermal choke has to be built through combustion organization, such that burned gas accelerates to supersonic and benefit RBCC performance. Much work has been completed in building a thermo choke in ramjet mode through matching in flight condition, flame sustaining, and secondary fuel injection distributing [10]. However significant differences in secondary burning organization exist between a ramjet- and ejector mode. In a ramjet mode, the inlet is start and incoming air is in control if the state of inlet unchanged. Furthermore it is also common in ramjet/scramjet mode to optimize a wide operating RBCC through a variable inlet geometry to match the incoming air with flow and combustion downstream. On a contrast, the inlet is un-start in ejector mode. A higher bypass ratio through an efficient ejection by rocket jet is favor for enhancing secondary burning so as to achieve a high pressure in the ramjet combustor and in turn to augment engine thrust. However a high pressure in the ramjet combustor may result in an overflow due to pressure travel upstream in the ramjet combustor. Hereby ejection is associated with complex coupling among flight condition, rocket jets, and secondary burning. Anyhow, it is important to achieve a steady secondary burning and appropriate thermo choke position such that thrust augmentation is realized. Hence it is necessary to study basis of secondary burning organization, thermo choke building and bypass ratio variation, and further to reveal mechanism of RBCC engine performance improvement in ejector mode.

In the paper three dimensional CFD of full flow path of RBCC and ground direct-connect experiments have been undertaken to study the effects of secondary fuel burning on the ejection and engine performance in ejector mode. Thermo choke, bypass ratio and engine performance have been compared by varying the injecting position and the equivalence ratio of the secondary fuel in an inner flow path configured for multiple modes.

2. Three dimensional CFD in whole flow path of RBCC

2.1. RBCC engine configuration

Three-dimensional CFD simulations have been completed in the whole flow path of RBCC including a fore- and aft-airframe of a flight vehicle. The RBCC is configured based on a typical centric strut as showed in Fig.1.

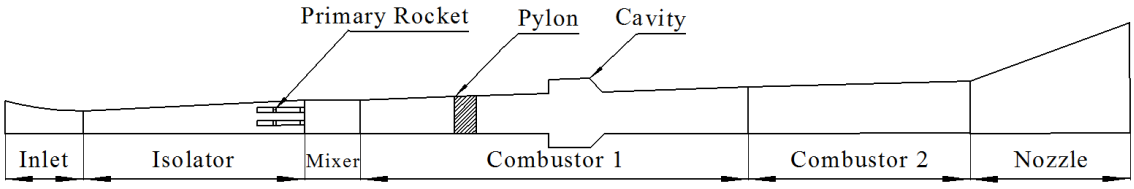

Fig 1. Configuration of RBCC for multiple modes

Bipropellant in the primary rocket is kerosene/liquid oxygen, while kerosene is also as the secondary fuel to burn with the incoming air. The primary rockets locate at the entrance to the mixer with a blockage ratio of 0.3. The ramjet-combustor consists of two slightly divergent sections with a hemi-expansion angle of 1.5°. The convergent ratio is 6.3 for fore-airframe with 2 stages compression while the expansion ratio of the aft-airframe nozzle is 1.5, which is favor for a scramjet mode as

mentioned above. The inlet starts at flight Ma 2.4. In order to lower drag force of the inlet and increase air mass flow rate, a bleeding is arranged in the throat of the inlet by opening or closing as necessary.

2.2. CFD method and verification

A set of equations represent mass, momentum and energy balance in gas and liquid phase, and species mass fraction in the flow and combustion is found in [9]. The N-S equation is solved based on finite volume method, and the continuous phase control equation and discrete phase control equation are established. The gas- and liquid phase control equations are described in the Euler coordinate system and Lagrange coordinate system, respectively. The interaction between droplet and gas phase is expressed by the source item of the interaction between gas phase and liquid phase when simulating the turbulent mixing and combustion of the primary and secondary flow with high momentum ratio.

The Shear Stress Transport (SST) k-ω model and cubic k-ε model are used. Wilcox k-ω model is for the near wall, while k-ε model for the shear layer. Schmidt- and Prandt numbers are taken as 0.5 and 0.9 respectively. Two step model for kerosene chemic kinetic and one step model for hydrogen are used. Total meshes are nearly 3600,000 in Fig.2. RBCC propelled flight vehicle with a wide envelop is characteristic of a highly integrated body frame with its propulsion device. The fore- and aft airframe of the vehicle are lift surfaces, and also aid to form the inlet and aft nozzle of RBCC functionally. Hence three-dimensional CFD simulations for RBCC whole inner flow path are usually completed including the fore- and aft-airframe of flight vehicle in order to involve the constrained flow effects on the inlet/exit of RBCC, though meshes hereby are vast increased. Verifications have been completed through comparisons with typical supersonic inlet flow fields obtained by striation technique [11], with ejector test, and with ground direct-connect experiments. More details are found in [12].

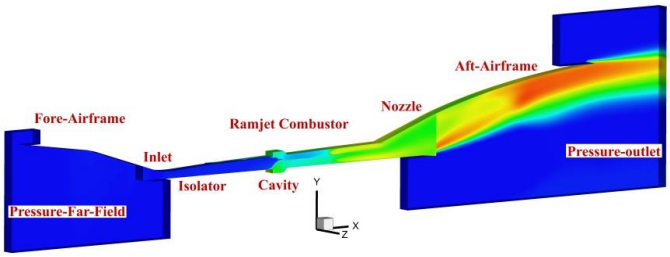

Fig 2. CFD domain of the whole flow path of RBCC

3. Simulation of Secondary burning organization and thrust augmentation

3.1. Thermal choke and Pressure profile in ram combustor

With increase of incoming air, secondary burning is organized through injected secondary fuel into a ram combustor and thus a specific impulse is increased. As shown in Fig. 1, the ram combustor consist of two sections, corresponding to the combustor 1 and combustor 2. Secondary fuel is injected solely through pylons, cavities arranged in combustor 1, poring holes on combustor 2, or through their combinations, such that a varied combustion organization is realized to obtain a stable secondary burning in a ram combustor. Under the same flight Ma and rocket jet operating parameters, combustion organization has been studied by varying fuel injecting distribution and thus the bypass ratio and engine performance can be compared.

At flight Ma2, the inlet is un-start and the primary rocket operates in a mass flow rate of 0.4kg/s. When a mixture ratio and nozzle expansion ratio taken as 2.9 and 6 respectively, the primary rocket chamber pressures is 4.7 MPa, while the total pressure ratio of primary jet to secondary flow is 23. Table 1 lists seven cases with varied fuel distributing. It is seen that the total secondary fuel equivalence ratio is 0.8 for all cases.

Fig. 3 shows the isothermal surface distribution of kerosene mass fraction. As shown in Fig. 3(a), secondary fuel from pylons in case FP-2-2 participates partly in the combustion in the center of the flow channel, and is drawn back partly into the cavity. For the ramjet combustor with one side expansion on the upper wall, the hot primary rocket jet with high temperature and the ejector air to the upper combustor wall create a high temperature environment and an oxygen-rich region, which is favor for the ignition and stable burning of the secondary fuel. It is seen that there is still a small amount of

secondary fuel remaining near the lower wall of the outlet of the ram combustor due to a poor mixing with incoming air.

Table 1. Secondary fuel injection position and equivalence ratio

Case	equivalence ratio of secondary fuel			Total equivalence ratio of secondary fuel
	At pylon	At cavity	In combustor 2	
FP-2-1	0	0	0	0
FP-2-2	0.8	0	0	0.8
FP-2-3	0	0.8	0	0.8
FP-2-4	0.4	0	0.4	0.8
FP-2-5	0	0.4	0.4	0.8
FP-2-6	0.2	0.2	0.4	0.8
FP-2-7	0	0	0.8	0.8

As shown in Fig. 3(b) for case FP-2-3, all of the secondary fuels are injected through the cavities, and fail to be mixed well with centric incoming air along the flow path due to a filmy penetration limited by cavities. The fuel is mainly concentrated in the rear edge of the cavity and results in a high local equivalent ratio near the cavities. The oxygen close to the upper and lower walls is completely exhausted, and the secondary fuel remained is still not burned out in the second combustor.

In case FP-2-4 and case FP-2-5, half of the secondary fuel is injected through pylons and the cavities respectively. The fuel through pylons in case FP-2-4 burns completely at the front edge of the cavity because of throughout mixing with incoming air, aided by pylons stretching. Also its rapid temperature rising near the centric high temperature rocket jet accelerates burning, compared to injection through cavities in case FP-2-5.

In case FP-2-6, the secondary fuel is distributed through the pylons, the cavities and the second combustor. It is found that the fuel into the first combustor is rapidly burned out because of a lower local equivalent ratio and also an enhancing mixing by pylons. Comparatively, distributing secondary fuel along the ram flow path is favor for its mixing and burning. In case FP-2-7, the secondary fuel is totally injected into the second combustor and its burning takes place in this section.

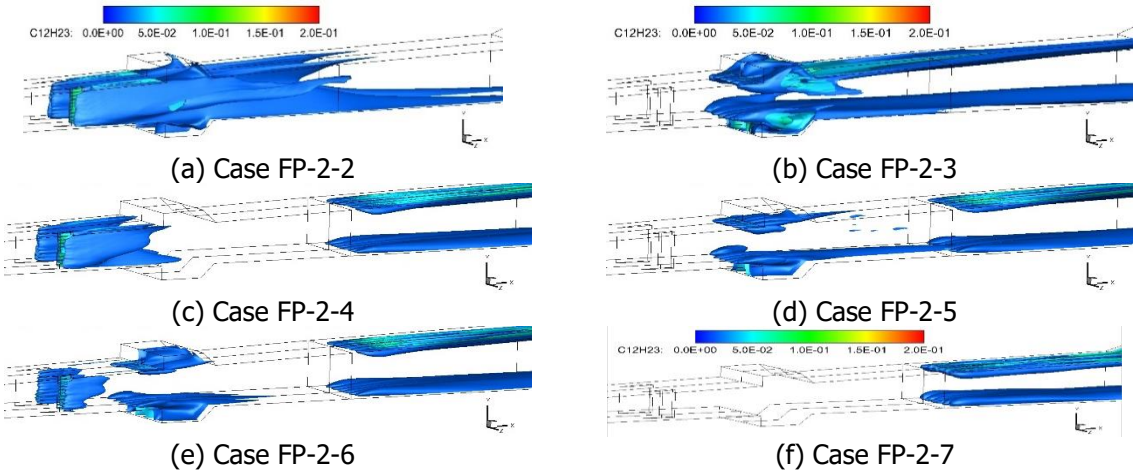

(a) Case FP-2-2 (b) Case FP-2-3

(c) Case FP-2-4 (d) Case FP-2-5

(e) Case FP-2-6 (f) Case FP-2-7

Fig 3. Isothermal surface distribution of kerosene mass fraction

In case FP-2-1, no secondary fuel is fed and a lowest mass-weighted average total temperature is observed in Fig. 4 due to absence of a secondary burning, though the increases of the total temperature along ram flow path is resulted from burning between fuel rich rocket jets and incoming air during their moving and mixing downstream. As seen in Fig.4 (a), the secondary burning brings an evident increase of total temperature of gas mixture in accord with secondary burning position. The

increase of total temperature of gas mixture for case FP-2-7 occurs far downstream, corresponding to a secondary burning taking place in the second combustor.

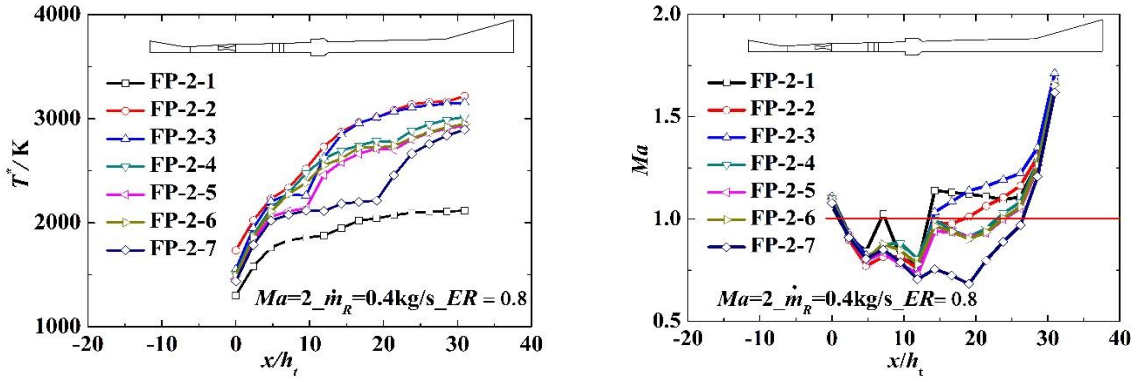

(a) Total Temperature (b) Ma

Fig 4. Mass-weighted average parameters of mixed gas flow along flow path under different secondary fuel injection distribution

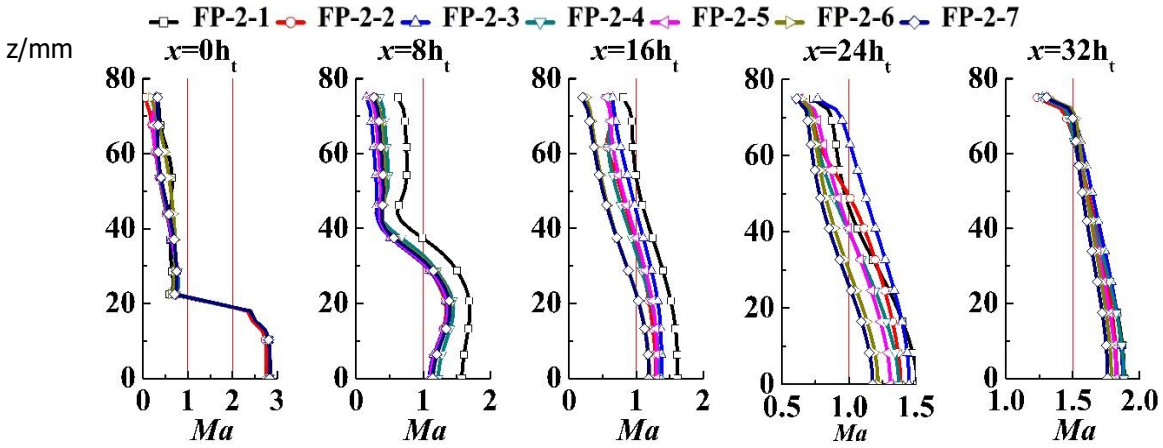

Fig 5. Ma of rocket jet at central cross-section under different secondary fuel distribution

The mass-weighted average gas mixture Ma profiles along flow path in Fig.4 (b) indicate comprehensive effects of momentum transfer between rocket jet and air flow, secondary burning organization and flow path configuration. A great momentum transfer between rocket jet and air flow results in mass-weighted average Ma decreasing from the rocket nozzle exit to front of pylons, as observed in Fig. 4(b). The momentum transfer between rocket jet and air flow has the rocket jet to decelerate along the whole flow path, such that Ma number of rocket jet centric (Z=0) decreases along x direction for all operation cases in Fig. 5. On contrast, a convergent flow path shaped by rear of cavity accelerates gas mixture in all operation cases such that mass -weighted average gas mixture achieves to supersonic after the cavity in case FP-2-1. However for other cases having secondary burning, their Ma profiles and thermo choke positions are dominated by secondary burning organization. Gas mixture decelerates on contrary due to secondary heat release until a thermo choke occurs adjoining the rear of cavities in case FP-2-2 and case FP-2-3 having fuel injected in the combustor 1. Afterwards for the two cases, the hot gas mixture with high total temperature expands in the slight divergent ram path until reaching the rear nozzle. For other rest cases, mass-weighted average gas mixture remains subsonic after the cavity, because the secondary heat release far downstream decelerates the gas mixture but fails to support it to expand afterwards. The gas mixture decelerates downstream until an accelerating effects of a secondary heat release is enough to results in a thermo choke. The thermo choke positions occur downstream successively along flow path for 5 cases with secondary burning, in accord with secondary heat release organizing positions downstream. The thermo choke occurs farthest for case FP-2-7 due to its secondary fuel totally injected into the combustor 2.

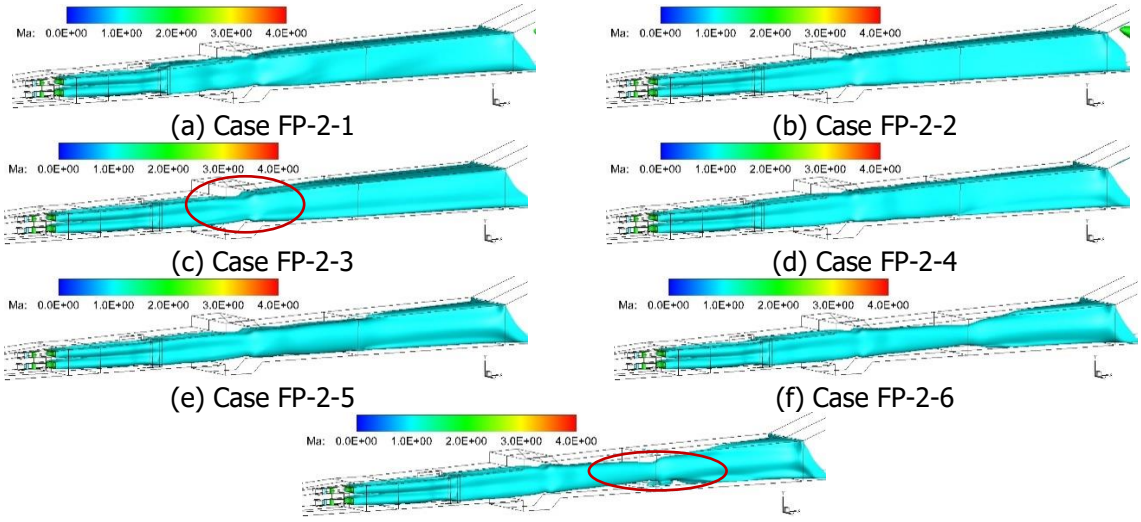

Fig 6. Equivalent distribution of Ma under different secondary fuel distribution

It is found that a stable secondary combustion is realized for all cases in an equivalence ratio of 0.8. And it is also possible to build a thermo choke downstream through controlling the fuel injection position. The equivalent distributions of Ma along ram flow path are shown in Fig. 6. Fig. 7 shows the pressure distribution of mass-weighted average gas flow along the ram flow path. The inlet suction groove remains open and the inlet throat pressure is close to the ambient pressure. A lowest pressure is shown for case FP-2-1 due to no secondary burning. The pressure in the combustor 1 is increased because of a secondary burning taking place near the pylons in case FP-2-2. However a lower ejection is resulted from an overflow in the inlet due to a high pressure traveling upstream. As seen in Table 2, the bypass ratio in case FP-2-2 is decreased by 29.4% of that in case FP-2-1. Anyhow the thrust in case FP-2-2 is increased by 9% because of its secondary burning, but unfortunately a lower ejection results in 6% decrease of specific impulse, compared to case FP-2-1.

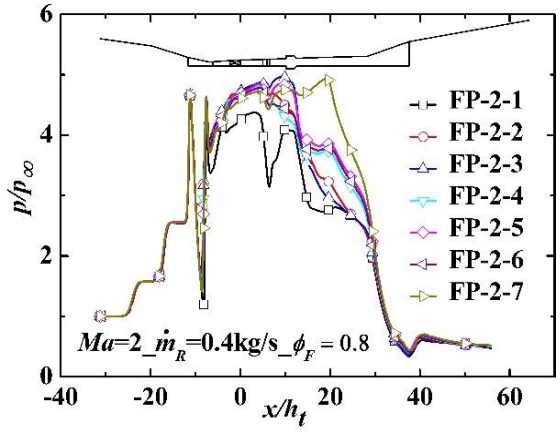

Fig 7. Pressure along flow path under different secondary fuel injection distribution

It is inspiring that overflow is attenuated and ejection is improved, when high pressure region moves downstream following the secondary burning organized downstream. That the bypass ratio in case FP-2-6 is situated as the second highest in Table 2 indicates that a distributing injection of fuels play an important role in ejection.

Higher thrust and also higher specific impulse achieve in case FP-2-7, which is resulted from matching of a high ejection and efficient secondary burning. A farthest downstream organized secondary burning has weak negative effects on overflow and hereby a high bypass ratio achieves. Also important is that a high pressure region in the combustor 2 together with a great pressure integral face contributes much to thrust augmentation. Hereby a higher specific impulse in case FP-2-7 is obtained because of high thrust enhancement in spite of a lower bypass ratio, compared to case FP-2-6.

Table 2. Engine performances under different secondary fuel injection distribution

Case	Airflow mass flow rate (kg/s)	Bypass ratio	Ratio of bypass ratio	Thrust ratio	Ratio of specific impulse
FP-2-1	1.382	3.46	β_A	F'_A	I'_A
FP-2-2	0.976	2.44	0.71 β_A	1.09 F'_A	0.94 I'_A
FP-2-3	0.986	2.47	0.71 β_A	1.11 F'_A	0.96 I'_A
FP-2-4	1.046	2.62	0.76 β_A	1.12 F'_A	0.97 I'_A
FP-2-5	1.108	2.77	0.80 β_A	1.15 F'_A	1.00 I'_A
FP-2-6	1.206	3.02	0.87 β_A	1.17 F'_A	1.02 I'_A
FP-2-7	1.144	2.86	0.83 β_A	1.19 F'_A	1.03 I'_A

It is evident that bypass ratio is not a sole seeking goal to achieve thrust augmentation, as shown in Table 2. Though ejector-ramjet effect increases with flight Ma and contributes to increasing bypass ratio before the inlet starts, pressure profile in the combustor plays also an important role in air ejection. High engine performances rely on an appropriate secondary burning organization, which far downstream thermo choke position interprets.

3.2. Secondary burning enhancing versus rocket throttling

Before the inlet starts, the primary rocket produces an engine thrust and meanwhile entrains air into the ram combustor to make secondary burning and hereby thrust enhancement possible. As studied in 3.1 section for RBCC operating at Ma2 with the same rocket jet and secondary fuel equivalent ratio, secondary combustion also affects the bypass ratio and engine performance through the position of the thermal throat and ramjet combustor pressure distribution. Therefore, matching between the incoming Ma, the primary rocket jet, and the secondary combustion is particularly important to improve engine performance. It arouses interests to reveal coupling characteristics in ejector mode when increasing the secondary fuel equivalent ratio versus rocket throttling to pursue an enhanced secondary combustion. For this purpose four cases are arranged in Table 3 in the flight state of Ma2. With throttling rocket flow rate from 0.8kg/s to 0.4kg/s, the secondary fuel equivalent ratio are set from 0.4 to 0.8, correspondingly to case ER-2-2 and ER-2-4. All fuels are injected into the combustor 2 in terms of the burning organization demands revealed in 3.1. For comparison, ER-2-1 and ER-2-3 are listed for rocket flow rate 0.8kg/s and 0.4kg/s respectively, but without secondary fuel injected.

Table 3. Rocket mass flow rate and secondary fuel equivalent ratio

Case	Mass flow rate of rocket (kg/s)	Chamber pressure of rocket (MPa)	Total pressure ratio of rocket jet to air flow	Secondary fuel equivalent ratio
ER-2-1	0.8	9.5	46	0
ER-2-2	0.8	9.5	46	0.4
ER-2-3	0.4	4.7	23	0
ER-2-4	0.4	4.7	23	0.8

The nozzle expansion ratio and mixture ratio of the primary rocket are taken as 3.4 and 6 respectively. When rocket mass flow rates set as 0.8kg/s and 0.4kg/s, the primary rocket chamber pressures are 9.5 MPa and 4.7 MPa, and as a result, the total pressure ratios of primary jet to secondary flow are 46 and 23 respectively.

Fig. 8 shows across section- and mass-weighted average total temperature and Ma distribution of the gas mixture. Since the primary rocket mixture ratio is increased to 3.4, the primary rocket jet temperatures and Ma numbers are higher for the cases in Table 3, compared to Fig. 4 with rocket

mixture ratio taken as 2.6. It is also shown that the mass-weighted average total temperature and Ma number of the gas mixture increase with the increase of the primary rocket mass flow rate, which is unfavorable to thermo choke building. No thermo choke occurs for case ER-2-1 and ER-2-3 because of no secondary burning organized. However no thermo choke for case ER-2-2 indicates that a weak secondary heat release downstream with a fuel equivalent ratio of 0.4 is not sufficient to decelerate the gas mixture having high Ma to subsonic when rocket flow rate is 0.8kg/s. A low engine specific impulse performance is thus unavoidable.

On contrast, the secondary heat release dominates RBCC with increasing of fuel equivalent ratio by means of throttling of rocket flow. Averaged gas mixture is decelerated with rocket flow rate decreasing to 0.4kg/s. Together with enhancing of secondary burning with fuel equivalent ratio increased to 0.8, then a thermo choke for case ER-2-4 is resulted. Fig.9 presents equivalent distribution of Ma along ram flow path. No obvious decelerating effects of secondary heat release on gas mixture flow for case ER-2-1 and case ER-2-2 with 0.8kg/s of rocket flow rate. Even if a secondary burning organized for case ER-2-2, a weak secondary heat release downstream fails to decelerate a powerful rocket jet and no thermo choke exist. With a fuel equivalent ratio increased to 0.8 and a throttled rocket jet at a flow rate of 0.4kg/s, supersonic flow shrinks evidently for case ER-2-4 due to enhanced decelerating by secondary heat release to a low Ma of gas mixture. Therefore it is possible to obtain performance improvement through matching of rocket flow rate and secondary fuel equivalent ratio, premising a thermo choke downstream.

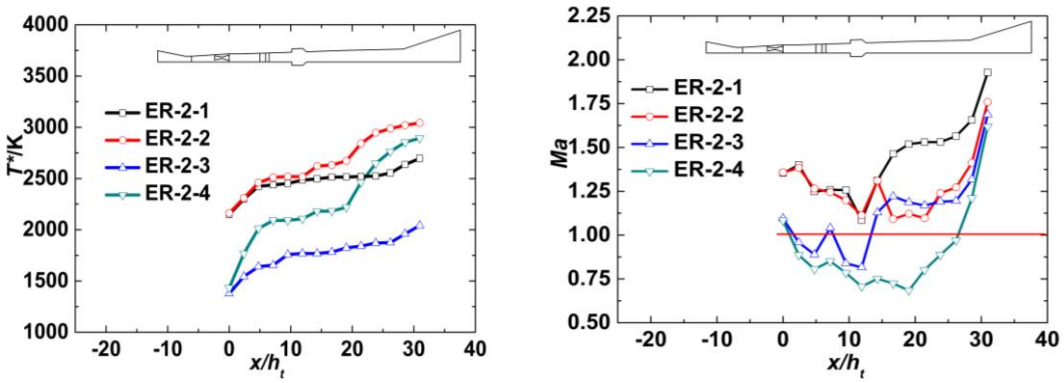

(a) Total Temperature (b) Ma

Fig 8. Mass-weighted average parameters of mixed gas flow along flow path versus rocket throttling

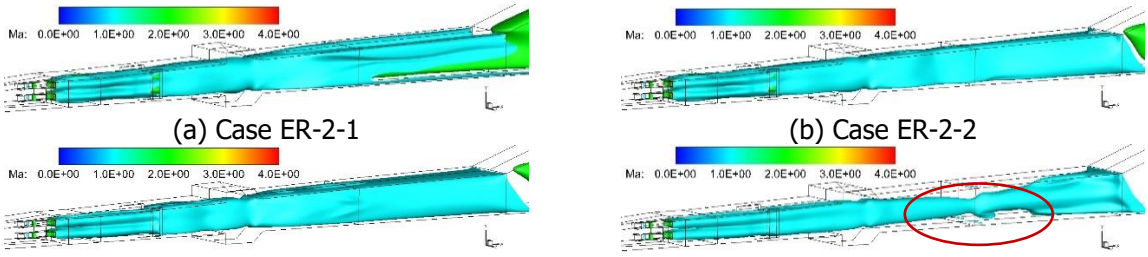

(a) Case ER-2-1 (b) Case ER-2-2

(c) Case ER-2-3 (d) Case ER-2-4

Fig 9. Equivalent distribution of Ma versus rocket throttling

Fig. 10 shows the pressure distribution along the ram flow path. The inlet suction groove remains open and the inlet throat pressure is close to the ambient pressure. When no secondary fuel injection, deeper throttling rocket jets for case ER-2-3 expands better in an under-expansion nozzle and exerts less crushing on incoming air. As a result, the bypass ratio for case ER2-2-3 is 2.32 as much as that for case ER-2-1, and more than 15.9% air flow is entrained into ram flow path. However their thrust and specific impulse are lower because of lack of thrust enhancing, compared to their corresponding cases having secondary burning with the same rocket flow rates, as shown in Table 4. The secondary burning brings performance improvements for case ER-2-2 and ER-2-4, though due to overflow effects by secondary burning, their bypass ratio decreases with 1.1% and 20.4%, compared to ER-2-1 and ER-2-3 respectively. Moreover case ER-2-4 is remarkable in increasing specific impulse, which indicates that increasing fuel equivalence ratio versus rocket throttling is feasible to improve specific impulse and thus

lower propellant consumption in ejector mode. That a higher thrust for case ER-2-2 with higher rocket flow rate and a higher specific impulse for case ER-2-4 with higher fuel equivalence ratio also indicates that matching of rocket flow rate and secondary fuel equivalence ratio is possible to achieve engine thrust demand, premising a high specific impulse.

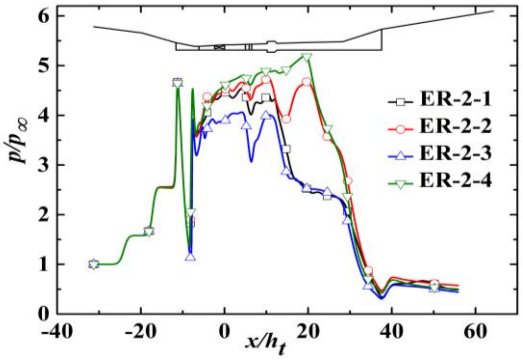

Fig 10. Pressure along flow path versus rocket throttling

Table 4. Influence of rocket throttling on engine performance

Case	Airflow mass flow(kg/s)	Bypass Ratio	Ratio of bypass ratio	Thrust ratio	Ratio of specific impulse
ER-2-1	1.249	1.56	β_B	F'_B	I'_B
ER-2-2	1.235	1.54	0.99 β_B	1.10 F'_B	1.06 I'_B
ER-2-3	1.448	3.62	2.32 β_B	0.61 F'_B	1.22 I'_B
ER-2-4	1.152	2.88	1.85 β_B	0.76 F'_B	1.28 I'_B

4. Ground direct-connect experiments

Ground direct-connect tests have been carried out to verify CFD simulation of secondary combustion heat release on the engine performance. In the experiments the inlet air flow and the outlet gases of the ramjet combustor were simulated by providing with an air heating mixer and an ejector back pressure chamber, respectively. The secondary burning is organized by varying the secondary fuel injection position and the ramjet combustor pressures have been measured.

4.1. Inlet and outlet airflow simulating

(a) Incoming air flow simulation

The ground direct- connect test system simulates the airflow entering the ram combustor by heating and mixing air with a hot gas from a gas generator. Fig.11 (a) shows the connection between the gas generator and the air mixing chamber. The air is heated and mixed in the mixing chamber with the hot gas out of the gas generator through a corrugated hose. After the mixing chamber, the mixed gas flows into the equipment nozzle section, where it is accelerated by the convergent-divergent expansion effect. The flow system provides an unchanged air flow rate during a test due to a great cost to adjust a throat area in the equipment nozzle section. Simulated air in the paper corresponds to exit of an inlet at Ma2 and 8 km altitude.

(b) High altitude simulation

A high-altitude back pressure environment has to be applied in the ground direct connect test in order to avoid an over-expansion of the gases in the aft nozzle. Compared to ramjet/scramjet mode of RBCC, it is nature that pressures in the ramjet combustor are lower in ejector mode of RBCC. In order to avoid the influence of back pressure in the ground environment on the flow and combustion in the ram combustor, an ejector's ejection suction has been used to simulate a back pressure at a high flight altitude. The back pressure keeps stable at 0.02 MPa. The connection between the engine outlet and the back pressure tank is shown in Fig. 11(b).

(a) Mixing cabin connection diagram

(b) back pressure tank connection

Fig 11. Inlet and outlet air flow simulating

4.2 Experiments results and discussion

The primary rocket propellants flow rate and mixture ratio are set as 0.12kg/s and 1.06 respectively, and the chamber pressure is 1.82MPa correspondingly. Incoming airflow rate, total pressure and total temperature are taken as 2.18 kg/s, 0.371 MPa and 385 K respectively. During each test, the incoming airflow parameters, back pressure of the ramjet combustor, and the primary rocket operating parameters remain unchanged.

Table 5 shows the arranged test cases with varied secondary fuel injection position and corresponding injection equivalent ratio during one test. Operation schedule for each case is also listed in Table 5. It takes the first 3s to reach a stable test conditions of simulated flight. In case Exp-p-1, the secondary fuel is injected in front of the cavity with an equivalent ratio 0.6 lasting 3s, corresponding to operating time 4s~7s. Thereafter, the fuel is organized injected lasting 1.5s through the cavity and the fuel pylon respectively, each at an equivalent ratio of 0.6. At the third case from 8.5s to 10.5s, the secondary fuel is injected at an equivalent ratio of 0.6 only at the cavity, meanwhile injection shut off at the pylon.

Table 5. Secondary fuel distribution and engine performance

Case	Secondary fuel injection position and equivalence ratio	Operating time(s)	Time averaged thrust increment(kN)
Exp-p-1	Cavity (0.6)	4~7	1.307
Exp-p-2	Pylon (0.6)+ Cavity (0.6)	7~8.5	1.991
Exp-p-3	Cavity (0.6)	8.5~10.5	1.228

It is found that a stable secondary burning is realized in turn during whole test of three cases with secondary fuel injection. Fig. 12 shows the measured pressure on the side of ramjet combustor along the flow path. For a comparison, a cold-flow test is also presented, in which only incoming air flows through the ramjet combustor. As showed in Table 5 and in Fig. 13, test cases having secondary burning present higher pressures and also higher thrust increments compared to the cold-flow test. The thrust increment is defined as the measured engine thrust during the direct-connect test minus that in the cold-flow test.

In case Exp-p-1, the highest pressure reaches 0.143MPa near the cavity, corresponding to its fuel injecting position. The high pressure in the ramjet combustor travels upstream, until reaching the primary rocket exit (8hc). The time averaged engine thrust increment in this case is 1.307KN, as shown in Fig. 13 and Table 5. With the increase of total equivalence ratio from 0.6 to 1.2 in Exp-p-2, higher pressures are shown in Fig. 12. Half the fuel is injected through pylon locating upstream of the cavity, and mixed well with the primary rocket jet and ejected airflow. As a result, a highest pressure is increased to 0.204MPa, increased by 42.7% compared to Exp-p-1. Also it is observed that pressure peak locates farther upstream than in Exp-p-1, which in accord with 3-D CFD simulations that secondary burning is influenced by fuel injection. The increased equivalence ratio and efficient burning

organization bring improvement of engine performance. As seen in Fig. 13, the time averaged thrust increment reaches 1.991KN and is increased by 52.3%, while its specific impulse is increased by 21.9% respectively, compared to Exp-p-1. In case Exp-p-3, the operation is as the same as Exp-p-1, when half of the secondary fuel through pylon is shut off. It is seen that the pressure profile and thrust increment are similar with case Exp-p-1.

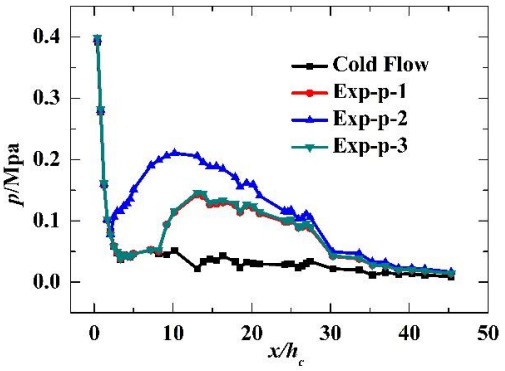

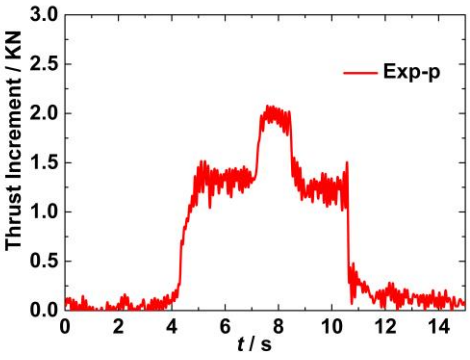

Fig 12 Measured pressure along flow path **Fig 13** Measured engine thrust increment

5. Conclusion

In the paper three dimensional CFD and ground direct-connect experiments have been undertaken aimed to study the effects of secondary fuel burning on the ejection and engine performance in ejector mode. The simulation results of the RBCC are in accord with ground direct-connect experiments. It is found that a stable secondary burning can be realized in an inner flow path configured for multiple modes of RBCC by injecting secondary fuel into ram combustor. A steady thermal choke have been realized through pylon and cavity aided combustion organization in a range of 0.4~0.8kg/s of rocket flow rate with an appropriate equivalence ratio at Ma2. The position of the thermal choke depends on secondary fuel distributing and plays a very important role in the thrust enhancement. A downstream injection of the secondary fuel into combustor 2 has its thermo choke built downstream and results in a less overflow of incoming air. Thus a higher specific impulse is obtained because of more entrained air and a great pressure integral face near aft-combustor. Matching of rocket flow rate and secondary fuel equivalence ratio is possible to achieve engine thrust demand, premising a high specific impulse through increasing secondary burning equivalence ratio by means of throttling primary rocket.

References

1. Gong C L, Han L. Optimization of ascent trajectory for RBCC-powered RLV. Journal of Solid Rocket Technology. 35(3), 290-295(2012)
2. Lin B, Pan H, Shi L, et al. Effect of Primary Rocket Jet on Thermodynamic Cycle of RBCC in Ejector Mode. International Journal of Turbo & Jet-Engines, (2017)
3. Etele J, Parent B, Sislian J P. Analysis of Increased Compression Through Area Constriction on Ejector-Rocket Performance. Journal of Spacecraft and Rockets, 44(2), 355-364(2007)
4. Koupriyanov M, Etele J. Theoretical Investigation of the Compression Augmentation Effects of Variable Area Ejectors. AIAA 2008-2619
5. Wisniewski C F, Heiser W H. Small-Scale Thrust Augmentation Analysis of Cold Flow Ejector/Diffuser Assembly. AIAA 2013-1067.
6. Kanda T, Kato K, Tani K, et al. Aerodynamic Characteristics of the Modified Combined Cycle Engines in Ejector-Jet Mode, AIAA 2006-223
7. Gist D R, Foster T J, DeTurris D J. Examination of Fabri-Choking in a Simulated Air Augmented Rocket. AIAA 2007-5392

8. Lear W E, Sherif S A, Parker G M. Effects of Fabri Choking on the Performance of Two-Phase Jet Pumps. AIAA 2000-3012
9. Pan H L, Lin B B, He G Q, et al. Effects of primary rocket pressure on ejection and combustion in RBCC configuration for multiple modes. J Propul Technol, 37(6):11108–11114(2016)
10. Wang Y J, Li J, He G Q, et al. Study of Strut-based RBCC Configuration to Improve Performance in Ramjet Mode. Journal of Solid Rocket Technology, 39(1): 9-16(2016)
11. Herrmann C D, Koschel W W. Experimental Investigation of The Internal Compression of a Hypersonic Intake[R]. AIAA 2002-4103.
12. Investigation on Matching of Operation of Primary Rocket with Whole Inner Passageway Bounded Flow and Thermodynamics in RBCC Ejector Mode. Xi'an China, Northwestern Polytechnical University, (2017)